

# Relativistic hyperpolarizabilities for atomic H, Li, and Be<sup>+</sup> systems

Shan-Shan Lu,<sup>1,2</sup> Hong-Yuan Zheng,<sup>1,2</sup> Zong-Chao Yan,<sup>3,1</sup> James F. Babb,<sup>4</sup> and Li-Yan Tang<sup>1,\*</sup>

<sup>1</sup> *State Key Laboratory of Magnetic Resonance and Atomic and Molecular Physics, Wuhan Institute of Physics and Mathematics, Innovation Academy for Precision Measurement Science and Technology, Chinese Academy of Sciences, Wuhan 430071, People's Republic of China*

<sup>2</sup> *University of Chinese Academy of Sciences, Beijing 100049, People's Republic of China*

<sup>3</sup> *Department of Physics, University of New Brunswick, Fredericton, New Brunswick, Canada E3B 5A3 and*

<sup>4</sup> *ITAMP, Center for Astrophysics | Harvard & Smithsonian, 60 Garden St., Cambridge, MA 02138, USA*

(Dated: November 20, 2023)

The hyperpolarizability of an atom is a property that describes the nonlinear interaction between an atom and an external electric field leading to a higher-order Stark shift. Accurate evaluations of these coefficients for various systems are crucial to improve experimental precision in advanced atom-based clocks. However, there is a dearth of reports on atomic hyperpolarizabilities, particularly regarding relativistic hyperpolarizabilities. Thus, in this paper, we use fourth-order perturbation theory to establish a universal formula for the hyperpolarizability and calculate the relativistic hyperpolarizabilities of low-lying states for the monovalent electronic atomic systems H, Li, and Be<sup>+</sup>. The highly accurate results given here for the H atom could serve as benchmarks for other theoretical methods.

PACS numbers: 31.15.ac, 31.15.ap, 34.20.Cf

## I. INTRODUCTION

The higher-order Stark shifts, which are characterized by hyperpolarizabilities, play a crucial role in suppressing nonlinear effects for precision spectroscopy measurements [1–4], especially in the pursuit and development of ever higher-precision optical clocks [5–9]. Regarding theoretical investigations, calculations of hyperpolarizabilities can be carried out in several ways, such as the Dalgarno-Lewis method [10], perturbation theory [11], finite-field approach [12], and finite-difference Hartree-Fock method [13]. Earlier work on atomic hyperpolarizabilities was reviewed by Thakkar and Lupinetti [14]. Some representative recent calculations can be found in Refs. [15–19]. For instance, Porsev *et al.* utilized the Dalgarno-Lewis method to determine the dynamic hyperpolarizabilities of Sr and Cd lattice clocks [15, 16]. Wu *et al.* performed calculations of the hyperpolarizabilities for clock states of Sr and Mg atoms by employing the sum-over-states method, which are consistent with the results of Porsev *et al.* within uncertainties for the Sr clock [17, 18]. Guo *et al.* employed the finite-field approach to calculate the static hyperpolarizabilities of the Cd atom [19]. Nevertheless, it is worth noting that theoretical calculations of relativistic hyperpolarizabilities for most atoms are currently inadequate or nonexistent so far.

Previous work conducted by Tang *et al.* [20] provided the detailed derivation of nonrelativistic hyperpolarizabilities, introducing the  $\delta(n, 0)$  function to handle the second term in the fourth-order energy correction  $\Delta E_4$ , as presented in Eqs. (A34) and (A35) of Ref. [20]. However, this treatment means that all quantum numbers must be the same between the intermediate state  $|n\rangle$  and the initial state, thereby ignoring the limitations on the magnetic quantum number  $M$ . In the present study, we used fourth-order perturbation theory to develop a universal formula for the relativistic hyperpolarizability without introducing  $\delta(n, 0)$ . To verify the correctness of formula, we conducted calculations for the low-lying states of the H, Li, and Be<sup>+</sup> systems. The hydrogen atom, being the simplest atomic system, was treated precisely by solving the Schrödinger and Dirac equations based on  $B$ -spline functions [21, 22]. For the Li atom and Be<sup>+</sup> ion, we employed the Dirac-Fock plus core polarization (DFCP) method to compute the relativistic hyperpolarizabilities of the low-lying states. The high-accuracy hyperpolarizabilities of the H atom could be useful benchmarks for testing the correctness of other methods. Atomic units are used throughout.

## II. FORMULA OF RELATIVISTIC HYPERPOLARIZABILITIES

When an atom is exposed to a uniform external electric field, the energy levels of the system undergo Stark shifts. The leading term is the second-order Stark shift related to the dipole polarizability, and the second term is the

---

\* Email Address: lytang@apm.ac.cn

fourth-order Stark shift related to the hyperpolarizability. The fourth-order Stark shift  $\Delta E_4$  can be written as:

$$\Delta E_4 = -\frac{\varepsilon^4}{24}\gamma = -\frac{\varepsilon^4}{24}\left\{\gamma_0 + g_2(J, M_J)\gamma_2 + [g_4(J, M_J)\gamma_4^{(1)} + g_2^2(J, M_J)\gamma_4^{(2)}]\right\}, \quad (1)$$

where  $\varepsilon$  is the electric field strength, the coefficients  $g_2(J, M_J)$  and  $g_4(J, M_J)$  depend on the magnetic quantum number  $M_J$ ,

$$g_2(J, M_J) = \begin{cases} 0, & J \leq \frac{1}{2}, \\ \frac{3M_J^2 - J(J+1)}{J(2J-1)}, & \text{otherwise}, \end{cases} \quad (2)$$

$$g_4(J, M_J) = \begin{cases} 0, & J \leq \frac{3}{2}, \\ \frac{3(5M_J^2 - J^2 - 2J)(5M_J^2 + 1 - J^2) - 10M_J^2(4M_J^2 - 1)}{J(2J-1)(2J-2)(2J-3)}, & \text{otherwise}, \end{cases} \quad (3)$$

In Eq.(1),  $\gamma_0$  corresponds to the scalar components of the second hyperpolarizability, whereas  $\gamma_2$ ,  $\gamma_4^{(1)}$ , and  $\gamma_4^{(2)}$  correspond to the tensor components, which have the following forms:

$$\gamma_0 = (-1)^{2J} \frac{24}{\sqrt{2J+1}} \sum_{J_a J_b J_c} \mathcal{G}_0^{(1)}(J, J_a, J_b, J_c) \mathcal{T}_1(J_a, J_b, J_c) - \frac{24}{2J+1} \sum_{J_a J_c} \mathcal{G}_{00}^{(2)}(J, J_a, J_c) \mathcal{T}_2(J_a, J_c), \quad (4)$$

$$\begin{aligned} \gamma_2 &= (-1)^{2J} 24 \sqrt{\frac{J(2J-1)}{(2J+3)(J+1)(2J+1)}} \sum_{J_a J_b J_c} \mathcal{G}_2^{(1)}(J, J_a, J_b, J_c) \mathcal{T}_1(J_a, J_b, J_c) \\ &\quad - \frac{24}{2J+1} \sqrt{\frac{J(2J-1)}{(2J+3)(J+1)}} \sum_{J_a J_c} [\mathcal{G}_{02}^{(2)}(J, J_a, J_c) + \mathcal{G}_{20}^{(2)}(J, J_a, J_c)] \mathcal{T}_2(J_a, J_c), \end{aligned} \quad (5)$$

$$\gamma_4^{(1)} = (-1)^{2J} 24 \sqrt{\frac{J(2J-1)(J-1)(2J-3)}{(2J+5)(J+2)(2J+3)(J+1)(2J+1)}} \sum_{J_a J_b J_c} \mathcal{G}_4^{(1)}(J, J_a, J_b, J_c) \mathcal{T}_1(J_a, J_b, J_c), \quad (6)$$

and

$$\gamma_4^{(2)} = -\frac{24J(2J-1)}{(2J+3)(2J+1)(J+1)} \sum_{J_a J_c} \mathcal{G}_{22}^{(2)}(J, J_a, J_c) \mathcal{T}_2(J_a, J_c), \quad (7)$$

where  $\mathcal{G}_\lambda^{(1)}(J, J_a, J_b, J_c)$  with  $\lambda = 0, 2, 4$  and  $\mathcal{G}_{k_1 k_2}^{(2)}(J, J_a, J_c)$  with  $k_1(k_2) = 0, 2, 4$  are defined in the Appendix A by Eqs. (A18) and (A19).

All relativistic formulas can be quickly transformed into nonrelativistic forms by replacing the total angular quantum number  $J$  with the orbital angular quantum number  $L$ , and the magnetic quantum number  $M_J$  with  $M_L$ .

### III. COMPUTATIONAL METHODS

#### A. Single-electron Schrödinger and Dirac equations

The Schrödinger equation for an atomic hydrogen of infinite nuclear mass is given by

$$\left[-\frac{1}{2}\nabla^2 + V(r)\right] \psi_S(\mathbf{r}) = E_S \psi_S(\mathbf{r}), \quad (8)$$

where  $V(r) = -1/r$ . Due to its rotational symmetry,  $\psi_S(\mathbf{r})$  can be separated into two factors

$$\psi_S(\mathbf{r}) = U_{nl}(r) Y_{lm}(\theta, \phi), \quad (9)$$

where  $Y_{lm}(\theta, \phi)$  is a spherical harmonic function and the radial function  $U_{nl}(r)$  satisfies the differential equation

$$\left[-\frac{1}{2} \frac{d^2}{dr^2} - \frac{1}{r} \frac{d}{dr} + \frac{l(l+1)}{2r^2} + V(r)\right] U_{nl}(r) = E_S U_{nl}(r). \quad (10)$$

The Dirac equation for hydrogen is given by

$$[c\boldsymbol{\alpha} \cdot \mathbf{p} + \beta m_e c^2 + V(r)]\psi_D(\mathbf{r}) = E_D \psi_D(\mathbf{r}), \quad (11)$$

where  $c = 137.035\,999\,074$  is the speed of light [23],  $m_e = 1$  is the electron mass,  $\mathbf{p}$  is the momentum operator, and  $\boldsymbol{\alpha}$  and  $\beta$  are the  $4 \times 4$  Dirac matrices [24]. The Dirac wavefunction is expressed as a spinor:

$$\psi_D(\mathbf{r}) = \frac{1}{r} \begin{pmatrix} i P_{n\kappa}(r) \Omega_{\kappa m}(\hat{\mathbf{r}}) \\ Q_{n\kappa}(r) \Omega_{-\kappa m}(\hat{\mathbf{r}}) \end{pmatrix}, \quad (12)$$

where  $P_{n\kappa}(r)$  and  $Q_{n\kappa}(r)$  are the large and small components of the radial function, and  $\Omega_{\kappa m}(\hat{\mathbf{r}})$  and  $\Omega_{-\kappa m}(\hat{\mathbf{r}})$  are the angular components. By substituting Eq. (12) into Eq. (11), we obtain the following coupled first-order differential equations that describe the behavior of  $P_{n\kappa}(r)$  and  $Q_{n\kappa}(r)$ :

$$\begin{pmatrix} V(r) & c \left( \frac{d}{dr} - \frac{\kappa}{r} \right) \\ -c \left( \frac{d}{dr} + \frac{\kappa}{r} \right) & -2m_e c^2 + V(r) \end{pmatrix} \begin{pmatrix} P_{n\kappa}(r) \\ Q_{n\kappa}(r) \end{pmatrix} = \varepsilon \begin{pmatrix} P_{n\kappa}(r) \\ Q_{n\kappa}(r) \end{pmatrix}, \quad (13)$$

where  $\varepsilon = E_D - m_e c^2$ .

Although both the Schrödinger equation Eq. (10) and the Dirac equation Eq. (13) can be solved analytically, in this study, we employ  $B$ -spline functions within a specified cavity [21, 22, 25, 26] to solve them numerically. This approach allows us to test our numerical procedure, which will later be applied to diagonalize the Hamiltonians. For instance, we can express  $U_{nl}(r)$  as a sum of  $N$ -dimensional,  $k$ -order  $B$ -spline basis functions:

$$U(r) = \sum_{i=1}^N c_i B_i^k(r), \quad (14)$$

where the subscripts  $n$  and  $l$  have been omitted for notational simplicity. The function  $B_i^k(r)$  is non-zero only within the knot intervals  $t_i \leq r \leq t_{i+k}$ , where  $\{t_i\}$  is the knot sequence. For the nonrelativistic and relativistic cases, the radial wave functions must satisfy the boundary conditions  $U(0) = U(R) = 0$ , and  $P(0) = 0$  and  $P(R) = Q(R)$ , respectively, where  $R$  is the radius of the cavity. In order to obtain accurate bound-state wave functions, it is more appropriate to use an exponential knot distribution for  $B_i^k(r)$  given by

$$t_{i+k-1} = R \times \frac{\exp \left[ \eta \left( \frac{i-1}{n-1} \right) \right] - 1}{\exp(\eta) - 1}, \quad i = 1, 2, \dots, N - k + 2. \quad (15)$$

Here,  $\eta = a \times R$  is an adjustable exponential knot parameter. In the present work, the radii of the confining cavity are fixed at  $R = 400$  a.u. and  $R = 600$  a.u. for nonrelativistic and relativistic calculations, respectively. The value of  $a$  is optimized by reproducing the exact energies [27] of low-lying states to about 20 significant digits.

## B. DFCP method

Since the Li atom and  $\text{Be}^+$  ion can be regarded as a frozen core combined with one valence electron, this system can be solved using the DFCP method. As described in previous studies [17, 28, 29], The DFCP method begins by performing a Dirac-Fock calculation of the frozen core. For monovalent electron systems, the effective Hamiltonian can be written as:

$$h_{\text{DFCP}}(\mathbf{r}) = c\boldsymbol{\alpha} \cdot \mathbf{p} + (\beta - 1)c^2 - (Z/r) + V_{\text{dir}}(r) + V_{\text{exc}}(r) + V_1(r). \quad (16)$$

Here,  $V_{\text{dir}}(r)$  and  $V_{\text{exc}}(r)$  represent, respectively, the direct and exchange potentials between the core electrons and the valence electron.  $V_1(r)$  is the semiempirical polarization potential, which can be expressed as:

$$V_1(r) = -\frac{\alpha_{\text{core}}}{2r^4} \left[ 1 - \exp \left( -\frac{r^6}{\rho_{\kappa}^6} \right) \right]. \quad (17)$$

The core dipole polarizabilities  $\alpha_{\text{core}}$  for  $\text{Li}^+$  and  $\text{Be}^{2+}$  are 0.1894 a.u. and 0.05182 a.u., respectively [30]. The cutoff parameter  $\rho_{\kappa}$  is adjusted to reproduce the experimental energies for the lowest state of each angular quantum number  $\kappa$ .

## IV. RESULTS AND DISCUSSIONS

### A. Hydrogen

Table I displays a convergence study for the nonrelativistic and relativistic hyperpolarizabilities,  $\gamma_0$ , of the ground state of the hydrogen atom. As the number of  $B$ -spline basis functions  $N$  varies from 100 to 400, the nonrelativistic value approaches the exact value of  $10665/8=1333.125$  a.u. [31]. Moreover, the relativistic result has been converged to 21 significant figures. The extrapolated value can be obtained by assuming that the ratio of two successive hyperpolarizability differences keeps constant as  $N$  becomes infinitely large. Comparing the nonrelativistic and relativistic values, we find that the relativistic correction on the hyperpolarizability of the ground state is  $-0.135\,342\,240\,736\,649\,84$  a.u.

For the nonrelativistic  $2p$  and  $3d$  states, the convergence of the calculations as the sizes of the  $B$ -spline basis sets increase are listed in Tables S1 and S2, and it can be seen that the converged values of the scalar and the tensor components have reached at least 21 significant digits. In particular, for the  $2p$  ( $|M_L| = 1$ ) state, the total hyperpolarizability  $\gamma$  is equal to  $5\,326\,848$  a.u., which is in perfect agreement with the result of Ref. [32].

In the relativistic case, the hyperpolarizabilities of  $2p_{1/2}$  and  $2p_{3/2}$  states, shown in Table S3, converged to 21 significant digits. Comparing with the nonrelativistic results, these values have significantly decreased due to the relativistic corrections, which are, respectively,  $-1079.819\,152\,938\,931\,31$  a.u. and  $-58.946\,729\,472\,921\,83$  a.u. for the scalar component  $\gamma_0$  of the  $2p_{1/2}$  and the  $2p_{3/2}$  states, and, respectively,  $-93.818\,725\,872\,360\,25$  a.u. and  $-1.166\,186\,367\,383\,566\,2$  a.u. for the tensor component  $\gamma_2$  and  $\gamma_4^{(2)}$  of the  $2p_{3/2}$  state. For the  $3d_{3/2}$  and  $3d_{5/2}$  states in Tables S4 and S5, they are converged to more than 19 significant digits, and the differences relative to the nonrelativistic  $\gamma_0$  are, respectively,  $-42\,365.011\,338\,2542$  a.u. and  $-10\,610.289\,081\,0328$  a.u. The tensor components  $\gamma_2$ ,  $\gamma_4^{(1)}$ , and  $\gamma_4^{(2)}$  of the  $3d_{5/2}$  state are close to the nonrelativistic results. All the final values of  $\gamma_0$ ,  $\gamma_2$ ,  $\gamma_4^{(1)}$ , and  $\gamma_4^{(2)}$  are summarized in Table II.

TABLE I: Convergence of the nonrelativistic and relativistic hyperpolarizability  $\gamma_0$  for the ground state of the H atom, in atomic units.

Nonrelativistic		Relativistic	
N	$\gamma_0$	N	$\gamma_0$
100	1 333.125 000 000 004	100	1 332.989 657 756
150	1 333.125 000 000 000 023	200	1 332.989 657 759 263 33
200	1 333.125 000 000 000 000 65	300	1 332.989 657 759 263 350 17
250	1 333.125 000 000 000 000 041	400	1 332.989 657 759 263 350 18
300	1 333.125 000 000 000 000 004 4	500	1 332.989 657 759 263 350 169
350	1 333.125 000 000 000 000 000 67	600	1 332.989 657 759 263 350 164
400	1 333.125 000 000 000 000 000 13	Extrap.	1 332.989 657 759 263 350 162
Ref. [31]	1 333.125		

TABLE II: Summary of relativistic and nonrelativistic hyperpolarizabilities for the low-lying states of the H atom, in atomic units. All the tabulated digits are insensitive to further enlargement of the  $B$ -spline basis functions. The numbers in the square brackets denote powers of ten.

State	$\gamma_0$	$\gamma_2$	$\gamma_4^{(2)}$	$\gamma_4^{(1)}$
Nonrelativistic				
$1s$	1333.125			
$2p$	8.130 560[6]	-2.769 472[6]	-3.424 0[4]	
$3d$	1.913 524 179 3[9]	-1.027 110 959 357 142 857 14[9]	-6.944 162 4[7]	2.939 248 330 714 285 714 2[7]
Relativistic				
$1s_{1/2}$	1 332.989 657 759 263 350 16			
$2p_{1/2}$	8.129 480 180 847 061 068 69[6]			
$2p_{3/2}$	8.130 501 053 270 527 078 17[6]	-2.769 565 818 725 872 360 25[6]	-3.424 116 618 636 738 356 62[4]	
$3d_{3/2}$	1.913 481 814 288 661 745 8[9]	-7.189 813 879 847 897 007[8]	-3.402 556 953 695 339 787 7[7]	
$3d_{5/2}$	1.913 513 569 010 918 967 2[9]	-1.027 113 325 161 422 291 3[9]	-6.944 098 825 526 105 146 0[7]	2.939 326 812 562 181 166 4[7]

### B. Li atom and Be<sup>+</sup> ion

In previous works, the nonrelativistic hyperpolarizabilities of the Li atom and Be<sup>+</sup> ion in low-lying states were calculated by using the Hylleraas variational method [20, 33]. Here we conduct single-electron calculations for the relativistic hyperpolarizabilities of the Li atom and Be<sup>+</sup> ion using a frozen-core Hamiltonian along with a semiempirical polarization potential. In the present calculation, we replace our energies with the corresponding NIST data [34], and consequently, the error bar in our results primarily arises from the reduced matrix elements. By comparing these matrix elements with the values in Ref. [35], we find that the relative differences for some reduced matrix elements are within 0.3% and 0.2% for the Li atom and Be<sup>+</sup> ion, respectively. To conservatively estimate the uncertainties in the relativistic hyperpolarizabilities of the Li atom and Be<sup>+</sup> ion, we introduce fluctuations of 0.3% and 0.2%, respectively, into all the reduced matrix elements.

The relativistic hyperpolarizabilities of the low-lying states for the Li atom and Be<sup>+</sup> ion are presented in Tables III. For the ground state  $2s_{1/2}$  of the Li atom, there exists a significant discrepancy between the present DFCP result of 5750 a.u. and the nonrelativistic Hylleraas result of 3060(40) a.u. [20], which can be attributed to a numerical cancellation. In the case of the hyperpolarizabilities of the  $2s_{1/2}$  state, they are determined as the sum of nine distinct types of intermediate states. These intermediate states can be further categorized based on their orbital angular quantum numbers, denoted as  $(m, n, k) = (mp_j, ns_{1/2}, kp_j)$  and  $(mp_j, nd_{j'}, kp_j)$ , where  $j = 1/2, 3/2$ ,  $j' = 3/2, 5/2$ , and  $|j - j'| \leq 1$ . The contributions from  $(mp_j, ns_{1/2}, kp_j)$  and  $(mp_j, nd_{j'}, kp_j)$  are  $-1\,469\,773$  a.u. and  $1\,475\,523$  a.u., respectively. As a result of this cancellation, there is a loss of three significant figures when combining the two contributions to obtain the total  $\gamma_0$ . Consequently, we can only provide the central value of 5750 a.u., which has the same order of magnitude as the nonrelativistic results. However, this situation does not arise in the ground state of the Be<sup>+</sup> ion. The contributions from  $(mp_j, ns_{1/2}, kp_j)$  and  $(mp_j, nd_{j'}, kp_j)$  amount to  $-20263$  a.u. and  $8755$  a.u., respectively, and their sum equals  $-11508(92)$  a.u., which is in good agreement with the all-order result of  $-11496(6)$  a.u. as reported in Ref. [36].

TABLE III: Summary of relativistic hyperpolarizabilities of the low-lying states for the Li atom and Be<sup>+</sup> ion, in atomic units. The numbers in parentheses and square brackets represent computational uncertainty and the power of 10, respectively.

State	$\gamma_0$	$\gamma_2$	$\gamma_4^{(2)}$	$\gamma_4^{(1)}$
Li				
$2s_{1/2}$	5750			
$2p_{1/2}$	9.82(12)[6]			
$2p_{3/2}$	9.82(12)[6]	$-6.126(74)[6]$	$1.439(17)[4]$	
$3d_{3/2}$	9.37(12)[11]	$-1.351(17)[12]$	$4.948(60)[11]$	
$3d_{5/2}$	9.37(12)[11]	$-1.930(23)[12]$	$1.009(13)[12]$	$-1.582(19)[10]$
Be <sup>+</sup>				
$2s_{1/2}$	$-11508(92)$			
Ref. [36]	$-11496(6)$			
$2p_{1/2}$	6647(54)			
$2p_{3/2}$	6650(53)	$-5237(42)$	$2134(17)$	
$3d_{3/2}$	5.952(48)[8]	$-9.081(73)[8]$	$3.730(30)[8]$	
$3d_{5/2}$	5.966(48)[8]	$-1.301(11)[9]$	$7.638(61)[8]$	$-5.835(47)[7]$

### C. Comparison of results under two different formulas

Remarkably, we find that despite significant differences in derivations of hyperpolarizabilities between the present work and previous work by Tang *et al.* [20], the total hyperpolarizabilities for each magnetic sublevel remain consistent. To explore the inherent differences between the two sets of formulas, we compared scalar and tensor hyperpolarizabilities for the  $2p$  state of the H, Li, and Be<sup>+</sup> systems, as shown in Fig. 1. It can be seen that for both scalar and tensor hyperpolarizabilities, the relativistic corrections obtained from the present formula are reasonable, while relativistic corrections calculated using the previous formula of Ref. [20] vary greatly.

As an example, we conduct a comprehensive analysis of the  $2p$  state in the Be<sup>+</sup> ion. According to the previous formula of Ref. [20], the nonrelativistic value of  $\gamma_0$  is  $10913.57(1)$  a.u., and the corresponding relativistic corrections are approximately  $-2130(70)$  a.u. ( $-20\%$ ) yielding  $8784(70)$  a.u. for the  $2p_{3/2}$  state and  $-4267(54)$  a.u. ( $-39\%$ ) yielding  $6647(54)$  a.u. for the  $2p_{1/2}$  state. In contrast, using the present formula, the relativistic corrections on  $\gamma_0$  fall within the error bars, and may be estimated as approximately 0.01% and 0.03%. Similarly, the relativistic correction on  $\gamma_2$

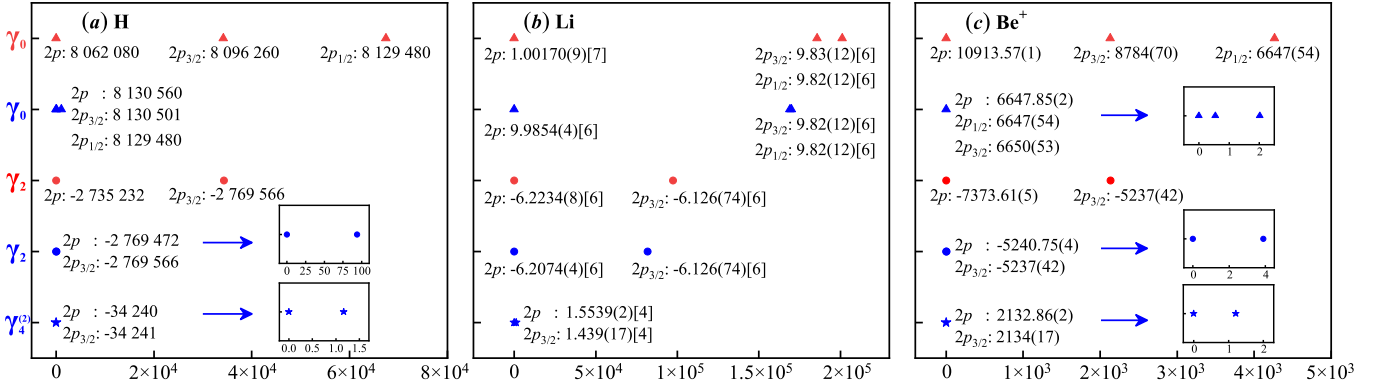


FIG. 1: (Color online) Comparison of relativistic corrections on the scalar and tensor hyperpolarizabilities for the  $2p$  state of the H, Li, and  $\text{Be}^+$  systems. The values in red or blue, respectively, are calculated using the previous formula from Ref. [20] or the present formula, while the terms  $\gamma_0$ ,  $\gamma_2$  and  $\gamma_4^{(2)}$ , respectively, are denoted by filled triangles, circles, and stars. All data are referenced to the nonrelativistic results on the far left, with the horizontal axis representing the absolute value of relativistic corrections. The inserts zoom in on the overlapping points within the main image. Note: the values of the H atom marked in the Fig. 2(a) only show the integers due to limited space.

using the previous formula is  $2137(42)$  a.u. (29%), which is significantly larger than the estimated 0.08% correction obtained from the present formula. These comparisons indicate that the present derivation is more reasonable in the allocation of scalar and tensor components of the hyperpolarizability than that found in the previous derivation [20], given that relativistic effects on physical properties are typically small corrections.

## V. SUMMARY

In summary, we have provided a complete derivation of the relativistic hyperpolarizability and established a universal formula without introducing  $\delta(n, 0)$ . The present formula can be easily converted to the nonrelativistic form. To validate the correctness of the present formula, we have calculated relativistic hyperpolarizabilities for low-lying states of the H, Li, and  $\text{Be}^+$  systems. These results can serve as benchmarks for testing other theoretical methods. In addition, the good agreement between relativistic and nonrelativistic values for excited states indicates that the present derivation is more reasonable in allocating scalar and tensor components of hyperpolarizability.

## Acknowledgments

This work was supported by the National Natural Science Foundation of China under Grant No. 12174402, and by the Nature Science Foundation of Hubei Province Nos.2019CFA058 and 2022CFA013. ZCY was supported by the Natural Sciences and Engineering Research Council of Canada (NSERC). JFB was supported in part by NSF grant PHY-2116679.

- 
- [1] B. M. Henson, J. A. Ross, K. F. Thomas, C. N. Kuhn, D. K. Shin, S. S. Hodgman, Y.-H. Zhang, L.-Y. Tang, G. W. F. Drake, A. T. Bondy, A. G. Truscott, and K. G. H. Baldwin, Measurement of a helium tune-out frequency: an independent test of quantum electrodynamics, *Science* **376**, 199 (2022).
  - [2] J. Yang, X. He, R. Guo, P. Xu, K. Wang, C. Sheng, M. Liu, J. Wang, A. Derevianko, and M. Zhan, Coherence preservation of a single neutral atom qubit transferred between magic-intensity optical traps, *Phys. Rev. Lett.* **117**, 123201 (2016).
  - [3] C. Sheng, X. He, P. Xu, R. Guo, K. Wang, Z. Xiong, M. Liu, J. Wang, and M. Zhan, High-fidelity single-qubit gates on neutral atoms in a two-dimensional magic-intensity optical dipole trap array, *Phys. Rev. Lett.* **121**, 240501 (2018).
  - [4] R. Guo, X. He, C. Sheng, J. Yang, P. Xu, K. Wang, J. Zhong, M. Liu, J. Wang, and M. Zhan, Balanced coherence times of atomic qubits of different species in a dual  $3 \times 3$  magic-intensity optical dipole trap array, *Phys. Rev. Lett.* **124**, 153201 (2020).



- [5] T. L. Nicholson, S. L. Campbell, R. B. Hutson, G. E. Marti, B. J. Bloom, R. L. McNally, W. Zhang, M. D. Barrett, M. S. Safronova, G. F. Strouse, W. L. Tew, and J. Ye, Systematic evaluation of an atomic clock at  $2 \times 10^{-18}$  total uncertainty, *Nat. Commun.* 6, 6896 (2015).
- [6] R. C. Brown, N. B. Phillips, K. Beloy, W. F. McGrew, M. Schioppo, R. J. Fasano, G. Milani, X. Zhang, N. Hinkley, H. Leopardi, T. H. Yoon, D. Nicolodi, T. M. Fortier, and A. D. Ludlow, Hyperpolarizability and operational magic wavelength in an optical lattice clock, *Phys. Rev. Lett.* 119, 253001 (2017).
- [7] I. Ushijima, M. Takamoto, and H. Katori, Operational magic intensity for Sr optical lattice clocks, *Phys. Rev. Lett.* 121, 263202 (2018).
- [8] S. Dörscher, J. Klose, S. Maratha Palli, and C. Lisdat, Experimental determination of the  $E2-M1$  polarizability of the strontium clock transition, *Phys. Rev. Res.* 5, L012013 (2023).
- [9] K. Kim, A. Aepli, T. Bothwell, and J. Ye, Evaluation of lattice light shift at low  $10^{-19}$  uncertainty for a shallow lattice Sr optical clock, *Phys. Rev. Lett.* 130, 113203 (2023).
- [10] A. Dalgarno and J. T. Lewis, The exact calculation of long-range forces between atoms by perturbation theory, *Proc. R. Soc. London A* 233, 70 (1955).
- [11] J. Mitroy, M. S. Safronova, and C. W. Clark, Theory and applications of atomic and ionic polarizabilities, *J. Phys. B* 43, 202001 (2010).
- [12] T. Fleig, Spin-orbit-resolved static polarizabilities of group-13 atoms: Four-component relativistic configuration interaction and coupled cluster calculations, *Phys. Rev. A* 72, 052506 (2005).
- [13] J. Kobus, D. Moncrieff, and S. Wilson, Comparison of the electric moments obtained from finite basis set and finite-difference hartree-fock calculations for diatomic molecules, *Phys. Rev. A* 62, 062503 (2000).
- [14] G. Maroulis, *Atoms, Molecules and Clusters in Electric Fields: Theoretical Approaches to the calculation of electric polarizability*, Imperial College Press, London (2006).
- [15] S. G. Porsev, M. S. Safronova, U. I. Safronova, and M. G. Kozlov, Multipolar polarizabilities and hyperpolarizabilities in the Sr optical lattice clock, *Phys. Rev. Lett.* 120, 063204 (2018).
- [16] S. G. Porsev and M. S. Safronova, Calculation of higher-order corrections to the light shift of the  $5s^2 \ ^1S_0 - 5s5p \ ^3P_0^o$  clock transition in Cd, *Phys. Rev. A* 102, 012811 (2020).
- [17] F.-F. Wu, Y.-B. Tang, T.-Y. Shi, and L.-Y. Tang, Dynamic multipolar polarizabilities and hyperpolarizabilities of the Sr lattice clock, *Phys. Rev. A* 100, 042514 (2019).
- [18] F.-F. Wu, Y.-B. Tang, T.-Y. Shi, and L.-Y. Tang, Magic-intensity trapping of the Mg lattice clock with light shift suppressed below  $10^{-19}$ , *Phys. Rev. A* 101, 053414 (2020).
- [19] X. T. Guo, Y. M. Yu, Y. Liu, B. B. Suo, and B. K. Sahoo, Electric dipole and quadrupole properties of the Cd atom for atomic-clock applications, *Phys. Rev. A* 103, 013109 (2021).
- [20] L.-Y. Tang, Z.-C. Yan, T.-Y. Shi, and J. F. Babb, Nonrelativistic ab initio calculations for  $2 \ ^2S$ ,  $2 \ ^2P$ , and  $3 \ ^2D$  lithium isotopes: Applications to polarizabilities and dispersion interactions, *Phys. Rev. A* 79, 062712 (2009).
- [21] W. R. Johnson, S. A. Blundell, and J. Sapirstein, Finite basis sets for the Dirac equation constructed from B splines, *Phys. Rev. A* 37, 307 (1988).
- [22] H. Bachau, E. Cormier, P. Decleva, J. E. Hansen, and F. Martín, Applications of B-splines in atomic and molecular physics, *Rep. Prog. Phys.* 64, 1815 (2001).
- [23] P. J. Mohr, B. N. Taylor, and D. B. Newell, CODATA recommended values of the fundamental physical constants: 2010, *Rev. Mod. Phys.* 84, 1527 (2012).
- [24] S. Kaneko, Relativistic corrections to the electric multipole polarizability and the shielding factor of a hydrogen-like ion, *J. Phys. B* 10, 3347 (1977).
- [25] C. F. Fischer and F. A. Parpia, Accurate spline solutions of the radial Dirac equation, *Phys. Lett. A* 179, 198 (1993).
- [26] L. Y. Tang, Y. H. Zhang, X. Z. Zhang, J. Jiang, and J. Mitroy, Computational investigation of static multipole polarizabilities and sum rules for ground-state hydrogen-like ions, *Phys. Rev. A* 86, 012505 (2012).
- [27] H. A. Bethe and E. E. Salpeter, *Quantum mechanics of one- and two-electron atoms*, Plenum, New York, 1977.
- [28] Y.-B. Tang, H.-X. Qiao, T.-Y. Shi, and J. Mitroy, Dynamic polarizabilities for the low-lying states of  $\text{Ca}^+$ , *Phys. Rev. A* 87, 042517 (2013).
- [29] J. Jiang, J. Mitroy, Y. Cheng, and M. W. J. Bromley, Relativistic semiempirical-core-potential calculations of  $\text{Sr}^+$  using laguerre and slater spinors, *Phys. Rev. A* 94, 062514 (2016).
- [30] W. Johnson, D. Kolb, and K.-N. Huang, Electric-dipole, quadrupole, and magnetic-dipole susceptibilities and shielding factors for closed-shell ions of the He, Ne, Ar, Ni ( $\text{Cu}^+$ ), Kr, Pb, and Xe isoelectronic sequences, *At. Data Nucl. Data Tables* 28, 333 (1983).
- [31] D. M. Bishop and J. Pipin, Calculation of the polarizability and hyperpolarizability tensors, at imaginary frequency, for H, He, and  $\text{H}_2$  and the dispersion polarizability coefficients for interactions between them, *J. Chem. Phys.* 97, 3375 (1992).
- [32] S. Cohen and S. I. Themelis, Numerical solution of Dalgarno-Lewis equations by a mapped Fourier grid method, *J. Chem. Phys.* 124, 134106 (2006).
- [33] L.-Y. Tang, J.-Y. Zhang, Z.-C. Yan, T.-Y. Shi, J. F. Babb, and J. Mitroy, Calculations of polarizabilities and hyperpolarizabilities for the  $\text{Be}^+$  ion, *Phys. Rev. A* 80, 042511 (2009).
- [34] A. Kramida, Yu. Ralchenko, J. Reader, and NIST ASD Team, NIST Atomic Spectra Database, version 5.10 (2022).
- [35] P. Barakhsan, A. Marrs, A. Bhosale, B. Arora, R. Eigenmann, and M. S. Safronova, Portal for High-Precision Atomic Data and Computation, version 2.0 (2022).
- [36] U. I. Safronova and M. S. Safronova, Relativistic many-body calculation of energies, lifetimes, polarizabilities, and hyperpolarizabilities in Li-like  $\text{Be}^+$ , *Phys. Rev. A* 87, 032502 (2013).

### Appendix A: Derivation of relativistic hyperpolarizability

The Hamiltonian of an atom under the influence of a weak external electric field is given by

$$H = H_0 + H' = H_0 - \boldsymbol{\varepsilon} \cdot \mathbf{d}. \quad (\text{A1})$$

Here,  $H_0$  is the atom's unperturbed Hamiltonian,  $\boldsymbol{\varepsilon}$  is the electric field strength, and  $\mathbf{d}$  is the atom's electric dipole moment, given by  $\mathbf{d} = -e\mathbf{r}$ , where  $\mathbf{r}$  is the electron's position vector relative to a laboratory frame. The perturbation,  $H'$ , can be expressed as  $\mathbf{r} \cdot \boldsymbol{\varepsilon}$  in atomic units.

According to perturbation theory, the fourth-order energy shift contains two terms:  $\Delta E_4^{(1)}$  and  $\Delta E_4^{(2)}$ :

$$\Delta E_4 = \Delta E_4^{(1)} + \Delta E_4^{(2)} = \sum_{mnk} \frac{\langle 0|H'|m\rangle \langle m|H'|n\rangle \langle n|H'|k\rangle \langle k|H'|0\rangle}{(E_0 - E_m)(E_0 - E_n)(E_0 - E_k)} - \sum_{mk} \frac{\langle 0|H'|m\rangle \langle m|H'|0\rangle \langle 0|H'|k\rangle \langle k|H'|0\rangle}{(E_0 - E_m)(E_0 - E_k)^2}. \quad (\text{A2})$$

Using the spherical tensor operator technique, we can expand  $H'|n\rangle \langle n|H'$  of Eq. (A2) as

$$H'|n\rangle \langle n|H' = \sum_{Kq} (-1)^{K+q} [r^{(1)} \otimes \lambda_n r^{(1)}]_q^K [\varepsilon^{(1)} \otimes \varepsilon^{(1)}]_{-q}^K, \quad (\text{A3})$$

where  $r_\mu^{(1)} = \sqrt{\frac{4\pi}{3}} r Y_{1\mu}$  and  $\lambda_n = |n\rangle \langle n|$ . Assuming that the external electric field  $\boldsymbol{\varepsilon}$  is linearly polarized parallel to the  $z$  axis, only the  $q = 0$  component exists in Eq. (A3). Thus we have

$$H'|n\rangle \langle n|H' = \sum_K (-1)^K \sqrt{2K+1} \sum_{q_1 q_2} \begin{pmatrix} 1 & 1 & K \\ q_1 & q_2 & 0 \end{pmatrix} r_{q_1}^{(1)} \lambda_n r_{q_2}^{(1)} [\varepsilon^{(1)} \otimes \varepsilon^{(1)}]_0^K. \quad (\text{A4})$$

Substituting Eq. (A4) into Eq. (A2),  $\Delta E_4^{(1)}$  and  $\Delta E_4^{(2)}$  can be written as

$$\begin{aligned} \Delta E_4^{(1)} &= \sum_{mnk} \sum_{k_1 k_2} \sum_{q_1 q_2 q_3 q_4} (-1)^{k_1+k_2} \sqrt{(2k_1+1)(2k_2+1)} \begin{pmatrix} 1 & 1 & k_1 \\ q_1 & q_2 & 0 \end{pmatrix} \begin{pmatrix} 1 & 1 & k_2 \\ q_3 & q_4 & 0 \end{pmatrix} [\varepsilon^{(1)} \otimes \varepsilon^{(1)}]_0^{k_1} [\varepsilon^{(1)} \otimes \varepsilon^{(1)}]_0^{k_2} \\ &\times \frac{\langle 0|r_{q_1}^{(1)}|m\rangle \langle m|r_{q_2}^{(1)}|n\rangle \langle n|r_{q_3}^{(1)}|k\rangle \langle k|r_{q_4}^{(1)}|0\rangle}{(E_0 - E_m)(E_0 - E_n)(E_0 - E_k)}, \end{aligned} \quad (\text{A5})$$

$$\begin{aligned} \Delta E_4^{(2)} &= - \sum_m \sum_{k_1} \sum_{q_1 q_2} (-1)^{k_1} \sqrt{2k_1+1} \begin{pmatrix} 1 & 1 & k_1 \\ q_1 & q_2 & 0 \end{pmatrix} \frac{\langle 0|r_{q_1}^{(1)}|m\rangle \langle m|r_{q_2}^{(1)}|0\rangle}{(E_0 - E_m)} [\varepsilon^{(1)} \otimes \varepsilon^{(1)}]_0^{k_1} \\ &\times \sum_k \sum_{k_2} \sum_{q_3 q_4} (-1)^{k_2} \sqrt{2k_2+1} \begin{pmatrix} 1 & 1 & k_2 \\ q_3 & q_4 & 0 \end{pmatrix} \frac{\langle 0|r_{q_3}^{(1)}|k\rangle \langle k|r_{q_4}^{(1)}|0\rangle}{(E_0 - E_k)^2} [\varepsilon^{(1)} \otimes \varepsilon^{(1)}]_0^{k_2}, \end{aligned} \quad (\text{A6})$$

where all the initial and intermediate states are simply denoted as  $|0\rangle = |n_0 J M_J\rangle$ ,  $|m\rangle = |m J_a M_a\rangle$ ,  $|n\rangle = |n J_b M_b\rangle$ ,  $|k\rangle = |k J_c M_c\rangle$ , with  $n_0$ ,  $m$ ,  $n$ , and  $k$  being the corresponding principal quantum numbers of states. The summation in Eqs. (A5) and (A6) over  $m$ ,  $n$ , and  $k$  actually represents the summation over all three sets of quantum numbers  $\{m, J_a, M_a\}$ ,  $\{n, J_b, M_b\}$ , and  $\{k, J_c, M_c\}$ .

By utilizing the Wigner-Eckart theorem to simplify Eqs. (A5) and (A6), we can arrive at the following expressions:

$$\Delta E_4^{(1)} = - \sum_{J_a J_b J_c} \sum_{k_1 k_2} (-1)^{k_1+k_2} \sqrt{(2k_1+1)(2k_2+1)} [\varepsilon^{(1)} \otimes \varepsilon^{(1)}]_0^{k_1} [\varepsilon^{(1)} \otimes \varepsilon^{(1)}]_0^{k_2} \mathcal{C}_1 \mathcal{T}_1(J_a, J_b, J_c), \quad (\text{A7})$$

$$\Delta E_4^{(2)} = \sum_{J_a J_c} \sum_{k_1 k_2} (-1)^{k_1+k_2} \sqrt{(2k_1+1)(2k_2+1)} [\varepsilon^{(1)} \otimes \varepsilon^{(1)}]_0^{k_1} [\varepsilon^{(1)} \otimes \varepsilon^{(1)}]_0^{k_2} \mathcal{C}_2 \mathcal{T}_2(J_a, J_c), \quad (\text{A8})$$

where  $\mathcal{T}_1(J_a, J_b, J_c)$  and  $\mathcal{T}_2(J_a, J_c)$  are radial-dependent terms, and  $\mathcal{C}_1$  and  $\mathcal{C}_2$  are the angular coefficients. The explicit expressions are as follows:



$$\mathcal{T}_1(J_a, J_b, J_c) = \sum_{mnk} \frac{\langle n_0 J \| r^{(1)} \| m J_a \rangle \langle m J_a \| r^{(1)} \| n J_b \rangle \langle n J_b \| r^{(1)} \| k J_c \rangle \langle k J_c \| r^{(1)} \| n_0 J \rangle}{[E_k(J_c) - E_{n_0}(J)] [E_m(J_a) - E_{n_0}(J)] [E_n(J_b) - E_{n_0}(J)]}, \quad (\text{A9})$$

$$\mathcal{T}_2(J_a, J_c) = \sum_m \frac{\langle n_0 J \| r^{(1)} \| m J_a \rangle \langle m J_a \| r^{(1)} \| n_0 J \rangle}{[E_m(J_a) - E_{n_0}(J)]} \sum_k \frac{\langle n_0 J \| r^{(1)} \| k J_c \rangle \langle k J_c \| r^{(1)} \| n_0 J \rangle}{[E_k(J_c) - E_{n_0}(J)]^2}, \quad (\text{A10})$$

$$\begin{aligned} \mathcal{C}_1 = & \sum_{M_a M_b M_c} \sum_{q_1 q_2 q_3 q_4} (-1)^{J-M_J+J_a-M_a+J_b-M_b+J_c-M_c} \begin{pmatrix} 1 & 1 & k_1 \\ q_1 & q_2 & 0 \end{pmatrix} \begin{pmatrix} 1 & 1 & k_2 \\ q_3 & q_4 & 0 \end{pmatrix} \begin{pmatrix} J & 1 & J_a \\ -M_J & q_1 & M_a \end{pmatrix} \\ & \times \begin{pmatrix} J_a & 1 & J_b \\ -M_a & q_2 & M_b \end{pmatrix} \begin{pmatrix} J_b & 1 & J_c \\ -M_b & q_3 & M_c \end{pmatrix} \begin{pmatrix} J_c & 1 & J \\ -M_c & q_4 & M_J \end{pmatrix}, \end{aligned} \quad (\text{A11})$$

$$\begin{aligned} \mathcal{C}_2 = & \sum_{M_a M_c} \sum_{q_1 q_2 q_3 q_4} (-1)^{J_a-M_a+J_c-M_c} \begin{pmatrix} 1 & 1 & k_1 \\ q_1 & q_2 & 0 \end{pmatrix} \begin{pmatrix} J & 1 & J_a \\ -M_J & q_1 & M_a \end{pmatrix} \begin{pmatrix} J_a & 1 & J \\ -M_a & q_2 & M_J \end{pmatrix} \begin{pmatrix} 1 & 1 & k_2 \\ q_3 & q_4 & 0 \end{pmatrix} \\ & \times \begin{pmatrix} J & 1 & J_c \\ -M_J & q_3 & M_c \end{pmatrix} \begin{pmatrix} J_c & 1 & J \\ -M_c & q_4 & M_J \end{pmatrix}. \end{aligned} \quad (\text{A12})$$

By using the graphical method of angular momentum, we can simplify  $\mathcal{C}_1$  and  $\mathcal{C}_2$ :

$$\mathcal{C}_1 = (-1)^{J-M_J} \left\{ \begin{matrix} 1 & 1 & k_1 \\ J & J_b & J_a \end{matrix} \right\} \left\{ \begin{matrix} 1 & 1 & k_2 \\ J & J_b & J_c \end{matrix} \right\} \sum_{\Lambda} (2\Lambda+1) \begin{pmatrix} J & J & \Lambda \\ -M_J & M_J & 0 \end{pmatrix} \begin{pmatrix} k_1 & k_2 & \Lambda \\ 0 & 0 & 0 \end{pmatrix} \left\{ \begin{matrix} k_1 & k_2 & \Lambda \\ J & J & J_b \end{matrix} \right\}, \quad (\text{A13})$$

$$\mathcal{C}_2 = \begin{pmatrix} J & J & k_1 \\ -M_J & M_J & 0 \end{pmatrix} \begin{pmatrix} J & J & k_2 \\ -M_J & M_J & 0 \end{pmatrix} \left\{ \begin{matrix} 1 & 1 & k_1 \\ J & J & J_a \end{matrix} \right\} \left\{ \begin{matrix} 1 & 1 & k_2 \\ J & J & J_c \end{matrix} \right\}. \quad (\text{A14})$$

Since  $\varepsilon$  is oriented along the  $z$  axis, we can express  $[\varepsilon^{(1)} \otimes \varepsilon^{(1)}]_0^k$  in the form:

$$[\varepsilon^{(1)} \otimes \varepsilon^{(1)}]_0^k = \sqrt{2k+1} \begin{pmatrix} 1 & 1 & k \\ 0 & 0 & 0 \end{pmatrix} \varepsilon^2. \quad (\text{A15})$$

By substituting Eqs. (A13), (A14), and (A15) into Eqs. (A7) and (A8), we obtain the final expressions for  $\Delta E_4^{(1)}$  and  $\Delta E_4^{(2)}$ :

$$\Delta E_4^{(1)} = -\varepsilon^4 \sum_{J_a J_b J_c} \mathcal{T}_1(J_a, J_b, J_c) \sum_{\lambda} (-1)^{J-M_J} \begin{pmatrix} J & J & \lambda \\ -M_J & M_J & 0 \end{pmatrix} \mathcal{G}_{\lambda}^{(1)}(J, J_a, J_b, J_c), \quad (\text{A16})$$

$$\Delta E_4^{(2)} = \varepsilon^4 \sum_{J_a J_c} \mathcal{T}_2(J_a, J_c) \sum_{k_1 k_2} \begin{pmatrix} J & J & k_1 \\ -M_J & M_J & 0 \end{pmatrix} \begin{pmatrix} J & J & k_2 \\ -M_J & M_J & 0 \end{pmatrix} \mathcal{G}_{k_1 k_2}^{(2)}(J, J_a, J_c), \quad (\text{A17})$$

where

$$\mathcal{G}_{\lambda}^{(1)}(J, J_a, J_b, J_c) = \sum_{k_1 k_2} (\lambda, k_1, k_2) \begin{pmatrix} 1 & 1 & k_1 \\ 0 & 0 & 0 \end{pmatrix} \begin{pmatrix} 1 & 1 & k_2 \\ 0 & 0 & 0 \end{pmatrix} \begin{pmatrix} k_1 & k_2 & \lambda \\ 0 & 0 & 0 \end{pmatrix} \left\{ \begin{matrix} 1 & 1 & k_1 \\ J & J_b & J_a \end{matrix} \right\} \left\{ \begin{matrix} 1 & 1 & k_2 \\ J & J_b & J_c \end{matrix} \right\} \left\{ \begin{matrix} k_1 & k_2 & \lambda \\ J & J & J_b \end{matrix} \right\} \quad (\text{A18})$$

$$\mathcal{G}_{k_1 k_2}^{(2)}(J, J_a, J_c) = (k_1, k_2) \begin{pmatrix} 1 & 1 & k_1 \\ 0 & 0 & 0 \end{pmatrix} \begin{pmatrix} 1 & 1 & k_2 \\ 0 & 0 & 0 \end{pmatrix} \left\{ \begin{matrix} 1 & 1 & k_1 \\ J & J & J_a \end{matrix} \right\} \left\{ \begin{matrix} 1 & 1 & k_2 \\ J & J & J_c \end{matrix} \right\}, \quad (\text{A19})$$

with the notation  $(\lambda, k_1, k_2) = (2\lambda+1)(2k_1+1)(2k_2+1)$ .

According to the properties of the  $3j$  symbol, the permissible values for  $k_1$  and  $k_2$  in Eqs. (A18) and (A19) are 0 and 2, while the permissible values for  $\lambda$  are 0, 2, and 4. Also using the following formulas:

$$(-1)^{J-M_J} \begin{pmatrix} J & J & 0 \\ -M_J & M_J & 0 \end{pmatrix} = (-1)^{2J} \frac{1}{\sqrt{2J+1}}, \quad (\text{A20})$$

$$(-1)^{J-M_J} \begin{pmatrix} J & J & 2 \\ -M_J & M_J & 0 \end{pmatrix} = (-1)^{2J} \frac{3M_J^2 - J(J+1)}{\sqrt{(2J+3)(J+1)(2J+1)J(2J-1)}}, \quad (\text{A21})$$

$$(-1)^{J-M_J} \begin{pmatrix} J & J & 4 \\ -M_J & M_J & 0 \end{pmatrix} = (-1)^{2J} \frac{3(5M_J^2 - J^2 - 2J)(5M_J^2 + 1 - J^2) - 10M_J^2(4M_J^2 - 1)}{\sqrt{(2J+5)(J+2)(2J+3)(J+1)(2J+1)2J(2J-1)(2J-2)(2J-3)}}, \quad (\text{A22})$$

the fourth-order energy shift  $\Delta E_4$  can finally be simplified in the form:

$$\Delta E_4 = \Delta E_4^{(1)} + \Delta E_4^{(2)} = -\frac{\varepsilon^4}{24} [\gamma^{(1)} + \gamma^{(2)}], \quad (\text{A23})$$

where

$$\gamma^{(1)} = \gamma_0^{(1)} + g_2(J, M_J)\gamma_2^{(1)} + g_4(J, M_J)\gamma_4^{(1)}, \quad (\text{A24})$$

$$\gamma^{(2)} = \gamma_0^{(2)} + g_2(J, M_J)\gamma_2^{(2)} + g_2^2(J, M_J)\gamma_4^{(2)}. \quad (\text{A25})$$

By denoting  $\gamma$  as the total hyperpolarizability, we obtain

$$\gamma = \gamma^{(1)} + \gamma^{(2)} = \gamma_0 + g_2(J, M_J)\gamma_2 + [g_4(J, M_J)\gamma_4^{(1)} + g_2^2(J, M_J)\gamma_4^{(2)}], \quad (\text{A26})$$

where  $\gamma_0 = \gamma_0^{(1)} + \gamma_0^{(2)}$ ,  $\gamma_2 = \gamma_2^{(1)} + \gamma_2^{(2)}$ , and the coefficients  $g_2(J, M_J)$  and  $g_4(J, M_J)$  depend also on the value of  $M_J$ :

$$g_2(J, M_J) = \begin{cases} 0, & J \leq \frac{1}{2}, \\ \frac{3M_J^2 - J(J+1)}{J(2J-1)}, & \text{otherwise}, \end{cases} \quad (\text{A27})$$

$$g_4(J, M_J) = \begin{cases} 0, & J \leq \frac{3}{2}, \\ \frac{3(5M_J^2 - J^2 - 2J)(5M_J^2 + 1 - J^2) - 10M_J^2(4M_J^2 - 1)}{J(2J-1)(2J-2)(2J-3)}, & \text{otherwise}, \end{cases} \quad (\text{A28})$$

The values of  $\gamma_0^{(1)}$  and  $\gamma_0^{(2)}$  correspond to the scalar components of the second hyperpolarizability, whereas  $\gamma_2^{(1)}$ ,  $\gamma_2^{(2)}$ ,  $\gamma_4^{(1)}$ , and  $\gamma_4^{(2)}$  correspond to the tensor components, which have the following forms:

$$\gamma_0^{(1)} = (-1)^{2J} \frac{24}{\sqrt{2J+1}} \sum_{J_a J_b J_c} \mathcal{G}_0^{(1)}(J, J_a, J_b, J_c) \mathcal{T}_1(J_a, J_b, J_c), \quad (\text{A29})$$

$$\gamma_2^{(1)} = (-1)^{2J} 24 \sqrt{\frac{J(2J-1)}{(2J+3)(J+1)(2J+1)}} \sum_{J_a J_b J_c} \mathcal{G}_2^{(1)}(J, J_a, J_b, J_c) \mathcal{T}_1(J_a, J_b, J_c), \quad (\text{A30})$$

$$\gamma_4^{(1)} = (-1)^{2J} 24 \sqrt{\frac{J(2J-1)(J-1)(2J-3)}{(2J+5)(J+2)(2J+3)(J+1)(2J+1)}} \sum_{J_a J_b J_c} \mathcal{G}_4^{(1)}(J, J_a, J_b, J_c) \mathcal{T}_1(J_a, J_b, J_c). \quad (\text{A31})$$

$$\gamma_0^{(2)} = -\frac{24}{2J+1} \sum_{J_a J_c} \mathcal{G}_{00}^{(2)}(J, J_a, J_c) \mathcal{T}_2(J_a, J_c), \quad (\text{A32})$$

$$\gamma_2^{(2)} = -\frac{24}{2J+1} \sqrt{\frac{J(2J-1)}{(2J+3)(J+1)}} \sum_{J_a J_c} [\mathcal{G}_{02}^{(2)}(J, J_a, J_c) + \mathcal{G}_{20}^{(2)}(J, J_a, J_c)] \mathcal{T}_2(J_a, J_c), \quad (\text{A33})$$

$$\gamma_4^{(2)} = -\frac{24J(2J-1)}{(2J+3)(2J+1)(J+1)} \sum_{J_a J_c} \mathcal{G}_{22}^{(2)}(J, J_a, J_c) \mathcal{T}_2(J_a, J_c). \quad (\text{A34})$$

In the nonrelativistic case, we only need to substitute the total angular quantum number  $J$  with the orbital angular quantum number  $L$ .

# Appendix B: Convergence test for excited states of the H atom

TABLE S1: Convergence of the nonrelativistic hyperpolarizabilities  $\gamma_0$ ,  $\gamma_2$ , and  $\gamma_4^{(2)}$  for the  $2p$  state of the H atom, in atomic units.

N	$10^{-6}\gamma_0$	$10^{-6}\gamma_2$	$10^{-4}\gamma_4^{(2)}$
100	8.130 559 999 999 999 42	-2.769 471 999 999 997 9	-3.423 999 999 999 996 7
150	8.130 559 999 999 999 996 5	-2.769 471 999 999 999 987	-3.423 999 999 999 999 981
200	8.130 559 999 999 999 999 899	-2.769 471 999 999 999 999 64	-3.423 999 999 999 999 999 47
250	8.130 559 999 999 999 999 993 5	-2.769 471 999 999 999 999 977	-3.423 999 999 999 999 999 966
300	8.130 559 999 999 999 999 999 30	-2.769 471 999 999 999 999 997 5	-3.423 999 999 999 999 999 996 4
350	8.130 559 999 999 999 999 999 89	-2.769 471 999 999 999 999 999 62	-3.423 999 999 999 999 999 999 45
400	8.130 559 999 999 999 999 999 98	-2.769 471 999 999 999 999 999 93	-3.423 999 999 999 999 999 999 89
Extrap.	8.130 560	-2.769 472	-3.424 0

TABLE S2: Convergence of the nonrelativistic hyperpolarizabilities  $\gamma_0$ ,  $\gamma_2$ ,  $\gamma_4^{(1)}$ , and  $\gamma_4^{(2)}$  for the  $3d$  state of the H atom, in atomic units.

N	$10^{-9}\gamma_0$	$10^{-9}\gamma_2$	$10^{-7}\gamma_4^{(1)}$	$10^{-7}\gamma_4^{(2)}$
100	1.913 524 179 299 999 1	-1.027 110 959 357 141 8	2.939 248 330 714 278	-6.944 162 399 999 999 0
150	1.913 524 179 299 999 995	-1.027 110 959 357 142 851	2.939 248 330 714 285 67	-6.944 162 399 999 999 994
200	1.913 524 179 299 999 999 85	-1.027 110 959 357 142 857 0	2.939 248 330 714 285 713	-6.944 162 399 999 999 999 85
250	1.913 524 179 299 999 999 991	-1.027 110 959 357 142 857 13	2.939 248 330 714 285 714 20	-6.944 162 399 999 999 999 990
300	1.913 524 179 299 999 999 999 0	-1.027 110 959 357 142 857 141 6	2.939 248 330 714 285 714 277	-6.944 162 399 999 999 999 999 0
350	1.913 524 179 299 999 999 999 85	-1.027 110 959 357 142 857 142 7	2.939 248 330 714 285 714 284	-6.944 162 399 999 999 999 999 85
400	1.913 524 179 299 999 999 999 97	-1.027 110 959 357 142 857 142 8	2.939 248 330 714 285 714 285	-6.944 162 399 999 999 999 999 97
Extrap	1.913 524 179 3	-1.027 110 959 357 142 857 143	2.939 248 330 714 285 714 29	-6.944 162 4

TABLE S3: Convergence of the relativistic hyperpolarizabilities  $\gamma_0$ ,  $\gamma_2$ , and  $\gamma_4^{(2)}$  for the  $2p_{1/2}$  and  $2p_{3/2}$  states of the H atom, in atomic units.

N	$2p_{1/2}$	$2p_{3/2}$		
	$10^{-6}\gamma_0$	$10^{-6}\gamma_0$	$10^{-6}\gamma_2$	$10^{-4}\gamma_4^{(2)}$
100	8.129 480 180 86	8.130 501 053 3	-2.769 565 818 76	-3.424 116 618 8
200	8.129 480 180 847 063	8.130 501 053 270 53	-2.769 565 818 725 875	-3.424 116 618 636 74
300	8.129 480 180 847 061 07	8.130 501 053 270 527 09	-2.769 565 818 725 872 368	-3.424 116 618 636 738 37
400	8.129 480 180 847 061 068 8	8.130 501 053 270 527 078 3	-2.769 565 818 725 872 360 4	-3.424 116 618 636 738 356 8
500	8.129 480 180 847 061 068 696	8.130 501 053 270 527 078 177	-2.769 565 818 725 872 360 260	-3.424 116 618 636 738 356 625
600	8.129 480 180 847 061 068 695	8.130 501 053 270 527 078 173	-2.769 565 818 725 872 360 258	-3.424 116 618 636 738 356 621
Extrap.	8.129 480 180 847 061 068 695	8.130 501 053 270 527 078 173	-2.769 565 818 725 872 360 258	-3.424 116 618 636 738 356 620

TABLE S4: Convergence of the relativistic hyperpolarizabilities  $\gamma_0$ ,  $\gamma_2$ , and  $\gamma_4^{(2)}$  for the  $3d_{3/2}$  state of the H atom, in atomic units.

N	$10^{-9}\gamma_0$	$10^{-8}\gamma_2$	$10^{-7}\gamma_4^{(2)}$
100	1.913 481 814 8	-7.189 813 884	-3.402 556 955
200	1.913 481 814 288 67	-7.189 813 879 847 99	-3.402 556 953 695 35
300	1.913 481 814 288 661 77	-7.189 813 879 847 897 25	-3.402 556 953 695 339 82
400	1.913 481 814 288 661 746	-7.189 813 879 847 897 011	-3.402 556 953 695 339 788
500	1.913 481 814 288 661 745 85	-7.189 813 879 847 897 007 3	-3.402 556 953 695 339 787 74
600	1.913 481 814 288 661 745 83	-7.189 813 879 847 897 007 1	-3.402 556 953 695 339 787 72
Extrap.	1.913 481 814 288 661 745 83	-7.189 813 879 847 897 007 1	-3.402 556 953 695 339 787 72

TABLE S5: Convergence of the relativistic hyperpolarizabilities  $\gamma_0$ ,  $\gamma_2$ ,  $\gamma_4^{(1)}$ , and  $\gamma_4^{(2)}$  for the  $3d_{5/2}$  state of the H atom, in atomic units.

N	$10^{-9}\gamma_0$	$10^{-9}\gamma_2$	$10^{-7}\gamma_4^{(1)}$	$10^{-7}\gamma_4^{(2)}$
100	1.913 513 569 3	-1.027 113 325 4	2.939 326 813 54	-6.944 098 826
200	1.913 513 569 010 93	-1.027 113 325 161 429	2.939 326 812 562 21	-6.944 098 825 526 12
300	1.913 513 569 010 918 99	-1.027 113 325 161 422 31	2.939 326 812 562 181 3	-6.944 098 825 526 105 18
400	1.913 513 569 010 918 967 6	-1.027 113 325 161 422 291 6	2.939 326 812 562 181 168	-6.944 098 825 526 105 146 5
500	1.913 513 569 010 918 967 30	-1.027 113 325 161 422 291 36	2.939 326 812 562 181 166 54	-6.944 098 825 526 105 146 03
600	1.913 513 569 010 918 967 29	-1.027 113 325 161 422 291 35	2.939 326 812 562 181 166 48	-6.944 098 825 526 105 146 01
Extrap.	1.913 513 569 010 918 967 29	-1.027 113 325 161 422 291 35	2.939 326 812 562 181 166 48	-6.944 098 825 526 105 146 01